Civil Engineering Infrastructures Journal xx,xx

DOI: 10.22059/ceij.2025.393248.2292

Rocking Concrete Shear Walls with Longitudinal-Perpendicular XADAS Dampers: Seismic Interaction with Moment Frames

F. Vahid-Vahdattalab[1], E. Ghandi[1,*], E. Shafei[2]

[1]*Faculty of Engineering, University of Mohaghegh Ardabili, Ardabil, Iran.*
f.vahdattalab@uma.ac.ir, https://orcid.org/0000-0002-6701-1623
[2]*Department of Civil Engineering, Urmia University of Technology, Urmia, Iran.*
e.shafei@uut.ac.ir, https://orcid.org/0000-0002-0975-2466
[*]*Corresponding Author, Ghandi@uma.ac.ir, https://orcid.org/0000-0001-7262-7898*

Received: 19/04/2025

Revised: 06/06/2025

Accepted: 01/08/2025

Abstract

This study explores the seismic interaction between a concrete moment-resisting frame and a rocking shear wall equipped with both longitudinal and perpendicular dampers. Unlike earlier works that placed dampers only along the wall's length, this research introduces transverse dampers mounted perpendicularly using brackets. A parametric study examined how damper cross-sections affect displacement, drift, acceleration, and overturning safety. CFRP tendon post-tensioning forces were adjusted to ensure self-centering, with 160 kN per tendon found optimal. Increasing this force beyond 160 kN offered no added benefit and could hinder wall uplift and energy dissipation, while lower forces weakened the self-centering effect. The structural response varied with damper cross-section. Unlike fixed-base systems where displacement consistently drops with larger dampers, rocking systems showed mixed trends. A 60×60 mm damper proved optimal for balancing displacement control and performance. Drift behavior followed conventional patterns, decreasing as damper size increased. A 245.45% drift reduction was observed with a 60×40 mm damper during the Kocaeli earthquake, but the 60×60 mm configuration with an M_R/M_O ratio of 0.93 was overall the most effective, combining stability and energy dissipation. Drift improvements became notable only after a specific damper size threshold, supported by time-history analysis from seven earthquakes. The study also found that the damper arrangement along the wall's edges significantly affects the overturning safety factor, particularly in rocking systems.

Keywords: Rocking Shear Wall, CFRP Tendons, Combined Damper Installation, XADAS Dampers, Time- History Analysis.

1. Introduction

Shear walls with fixed bases have been extensively utilized in concrete structures due to their acceptable performance. Residual drift and permanent deformations in buildings following severe earthquakes, along with economic considerations regarding repair costs, advancements in technology, and deeper research, have driven many researchers to develop sustainable structural systems with self-centering characteristics. Consequently, rocking shear walls have entered into opposition with their fixed-base counterparts. The interaction between moment frames and shear walls, especially the rocking type, has always been a challenging topic. This is primarily because rocking shear walls cannot be directly modeled in software like ETABS. Therefore, examining the interaction between frames and rocking shear walls in finite element software is of particular importance. Rocking shear walls, by themselves, do not have the capability to dissipate energy. Naturally, due to the use of tendons, these walls only exhibit self-centering properties. Hence, they must be combined with energy-dissipating systems (fuses). Types of energy-dissipating systems include internal fuses, external fuses, and dampers. Huang et al. conducted a study titled analytical investigation on lateral load responses of self-centering walls with distributed vertical dampers. The study found that variations in damper stiffness have minimal impact on the lateral load response of the wall. Additionally, increasing the initial stress in PT (post-tensioning) tendons enhances the SC ratio and lateral resistance at the ELL (effective limit of the linear-elastic response of the wall) point but makes the wall more susceptible to tendon yielding as the lateral load increases (Huang et al., 2019). Rocking systems are replaceable, as the tendons used can be easily replaced after an earthquake if they experience rupture or relaxation. Research by Lv et al. (2021), titled experimental and analytical study on cross-laminated bamboo (CLB) rocking walls with friction dampers, demonstrated that the hysteretic curves of the CLB rocking wall exhibit bilinear behavior. The stiffness inflection points remained nearly constant across seven tests, and the CLB wall stayed elastic throughout the loading process. This suggests that the stiffness inflection point arises from the reduction in the contact length between the CLB wall and the foundation.
A parametric study on pre-stressed concrete frame structures with variable friction dampers, conducted by Huang et al. (2023), revealed two methods to enhance the secondary stiffness of SCPC (self-centering pre-stressed concrete) joints (primarily determined by the stiffness of the pre-stressed strands): increasing the stiffness (or number) of the pre-stressed strands and extending the force arm of the pre-stressed strands. At the DBE (design-basis earthquakes) seismic level, enhancing secondary stiffness had limited effectiveness in reducing structural deformations, while at the MCE (maximum-considered earthquakes) seismic level, the impact was significant. The method of increasing the number of pre-stressed strands may raise economic costs, whereas extending the force arm of the strands is easily implementable and more cost-effective. Palnikov (2017), in his study titled design and experimental investigation of seismic retrofitting of electric transmission transformers using rocking structures and supplemental self-centering damping, concluded that retrofitted systems exhibited a 25–40% reduction in base frequency compared to non-retrofitted cases. Zhong et al. (2024) conducted a seismic performance study of a novel rocking joint based on a hemisphere, leading to a damage-free self-centering bridge system, demonstrated that the proposed design ensures the HRH (hemisphere-based rocking hinge) column remains anchored to the foundation under service loads, maintains a damage-free response, and provides sufficient energy dissipation capacity at target drifts while retaining its self-centering ability. Zhang et al. (2024) demonstrated in their study that RAC (recycled aggregate concrete) shear walls confined with steel tubes showed a 19% increase in lateral strength and a 77% increase in cyclic energy dissipation. When the steel tube casing developed micro-cracks, it had minimal impact on the overall cyclic behavior. An increase in the axial load ratio enhanced both lateral strength and energy dissipation capacity, while other experimental variables, such as concrete compressive

strength and confinement type, had minor effects. The addition of steel fibers also improved the mechanical properties of the concrete and reduced damage to the bases of the tested walls.

The results of a study with the title novel pre-pressure friction spring RC rocking column with enhanced segment by Ding et al. (2024) showed that the designed PFSRC (pre-pressure friction spring rocking column) exhibited comparable strength and stiffness to a fixed-base column under service-level earthquakes. Under design-level earthquakes, the pre-yield stiffness of the PFSRC was higher than that of the fixed-base column. When the friction spring was activated, its stiffness became lower than that of the fixed-base column. However, due to the absence of stiffness degradation, its ultimate load-bearing capacity was similar to that of the fixed-base column, while its energy dissipation capacity was lower. The results of the study by Wang et al. (2022) indicated that DVBF (dual-self-centering variable friction braced frame) could withstand six levels of vibration intensity without local buckling or frequency reduction, with a maximum PGA (peak ground acceleration) exceeding 1.2g. Although the maximum frame drift exceeded 2.5%, the braces and frame returned to their initial positions with minimal residual drifts.

Xue et al. (2021) conducted a study about development of a novel self-centering slip friction brace for enhancing the cyclic behaviors of RC double-column bridge bents. The results showed that the design of the SCSF (self-centering slip friction) brace is straightforward, with a clear working mechanism. The brace can be easily assembled in a factory or on-site and can be applied to both new bridges and retrofitted ones. A study titled multi-objective design method for seismic retrofitting of existing reinforced concrete frames using pin-supported rocking walls by Chen et al. (2022) demonstrated that this method is practical and can be utilized for the preliminary design of such structures. Han et al. (2023), in their study around design and numerical analysis of CLB buildings with different rocking wall configurations, concluded that the DBD (displacement-based design) of CLB rocking walls identifies key parameters such as initial pre-stress and cross-sectional area of PT (pre-stressed tendons), as well as the frictional force of the conventional friction damper (CFD). The elastic deformation of the wall panels, which was neglected in the initial design, was revisited during the verification stage. Vahid-Vahdattalab and Ghandi (2024), in their study about seismic performance analysis of rocking shear walls with high-strength concrete and perpendicular dampers, concluded that increasing the compressive strength of concrete leads to a reduction in the dimensions of the wall and, consequently, its weight. While this effectively contributes to the development of self-centering properties, it does not enhance energy dissipation. The findings of a study under the title of self-centering structures against earthquakes revealed that the first and perhaps most widespread SC approach involved the use of PT tendons. However, accurately predicting the initial stiffness of SC members based on PT remains a challenge in practice. Small strains induced by PT tendons must be considered when designing an SC member. For FRP tendons, potential sudden and brittle failure mechanisms should also be carefully addressed (Fang et al., 2023).

The self-centering behavior of rocking concrete walls equipped with high-yield-capacity yielding dampers, which provide ductile cyclic behavior with negligible residual deformations, has consistently been a focus of recent studies. One key question is the performance of such systems when combined with XADAS (x shape adding damping and stiffness) dampers placed on both sides of the wall bases. Additionally, since the behavior of concrete rocking walls combined with XADAS dampers involves imposing a vibration mode with a linear distribution along the height of the structure while controlling deformation levels, the ratio of damper capacity to the design seismic base shear prescribed by the code must be carefully considered. The objective of this study is to present a numerical computational framework for estimating the behavior of reinforced concrete moment frames designed according to the ASCE7-10 (ASCE7, 2010) seismic code and for passively controlling their motion using a combination of self-centering rocking walls with XADAS dampers. This parametric investigation examines the effects of earthquake frequency range and plastic capacity of the dampers on maximum displacement thresholds, inter-story drift, and acceleration distribution along the height of the structure. The results provide preliminary recommendations for designing these innovative seismic control systems. The results of the study by Aydin et al. (2019) indicated

that dampers should be optimally placed within the structure. Compared to uniform designs, optimal designs yield better performance in terms of displacement, acceleration, and base shear force. In their study on the optimal design and distribution of viscous dampers for shear building structures under seismic excitations, Cetin et al. (2019) concluded that optimally designed and placed VDs (viscous dampers) can effectively reduce the amplitudes of the transfer function. Ghandi et al. (2025) concluded that columns with lower aspect ratios exhibit greater maximum displacements but lower peak impact forces. Their study demonstrated that as the cross-sectional aspect ratio increases, the peak impact force rises while the maximum displacement decreases.

2. Modeling and Research Methodology

2.1. Preliminary Design of Moment Frames and Shear Walls

For the modeling of the 3D structure of a 9-story intermediate ductility moment frame, the software (ETABS, 2016) was used. After simulating the structural model and designing it, as well as determining the dimensions of the moment frame sections, one of the spans was selected for the implementation of the rocking shear wall and the subsequent installation of longitudinal and perpendicular dampers. This span was then transferred to SeismoStruct (2022) for two-dimensional time-history analysis. In SeismoStruct, the definition of elements and materials tailored to the research needs follows a specific process. As is known, the ETABS software is not suitable for nonlinear seismic analysis of structures. In line with this understanding, all nonlinear dynamic analyses were conducted using the powerful macro-FEM software SeismoStruct, which is based on a force-based formulation, unlike the conventional displacement-based formulations in ETABS. It should be noted that ETABS was used solely for determining the cross-sectional dimensions of the designed structure. For this purpose, seven accelerogram records were initially selected. After scaling all of them in accordance with relevant standards, the earthquake loads were applied to the structure under study, and nonlinear time history dynamic analysis was performed using the SeismoStruct software.

Reputable seismic codes emphasize the importance of three-dimensional analyses, particularly within the context of performance-based seismic evaluation. In this study, the analysis was limited to a specific plane (e.g., X or Y direction) to investigate the behavior and effectiveness of the damper, considering that rocking shear walls typically act in a single direction due to their uplift mechanism. This approach is commonly accepted as a preliminary step in the design and assessment of structural control systems, allowing for clearer interpretation of influential parameters and enabling sensitivity analyses. It also serves as a foundation for developing more comprehensive three-dimensional models in future phases of analysis or design. Numerous previous studies on damping systems have similarly employed two-dimensional models during early stages to better control variables and gain deeper insight into system behavior. Additionally, because rocking shear walls function unidirectionally, a bidirectional response would require an L-shaped or U-shaped configuration, in which case three-dimensional analysis becomes essential. However, since the rocking shear walls in this investigation were modeled as unidirectional elements, a two-dimensional analysis was considered sufficient for the intended scope and objectives.

The materials used for the rocking shear wall and moment frame are of the type Con_ma, as proposed by Mander et al. (1988). To calculate the modulus of elasticity for concrete, the Eq. (1) has been employed, where f_c' represents the compressive strength of concrete, and W_c denotes the specific weight of concrete.

$$E_c = 0.043 W_c^{1.5} \sqrt{f_c'} \quad (1)$$

The Stl_mp material, suggested by Menegotto and Pinto (1973), has been used to model the dampers and reinforcements. Additionally, El_Mat material has been utilized for modeling the CFRP tendons. The cross-sections of all elements in the 2D structure have been modeled using the Fiber Section approach. Furthermore, all structural components, except for the tendons, have been modeled using the Inelastic

Plastic Hinge Force-Based Element, while the tendons have been modeled as Inelastic Truss Elements. For more details, refer to the study by Vahid-Vahdattalab and Ghandi (2024). The dimensions of the designed sections for the 9-story structure in ETABS are presented in Table 1. Additionally, the structural plan is shown in Figure 1. The structure is intended for residential use, with a floor-to-floor height of 3.2 meters. Floors are considered rigid diaphragms, with two-way slabs of 20 cm thickness. The seismic lateral loading of the structure was applied according to the ASCE 7-10 code, and other details, including the response modification factor (R), the system over strength factor (Ω), the displacement amplification factor (C_d), the importance factor (I), and the Site Class, are reported in Table 2. The type of lateral load-resisting system before adding the rocking shear wall in both main directions was considered an intermediate ductility reinforced concrete moment frame. P-Δ effects were included, and the design of the concrete members was conducted using the CSA A23.3-14 code (CSA A23.3, 2014). Additionally, the fundamental period of the structure (T), based on ASCE 7-10, is 0.96 seconds.

Table 1: Details of the Sections for the 9-Story Structure

Story	Columns		Dimension and Reinforcement of X Axis Beams		
	Size (mm)	Rebar (mm)	Size (mm)	Upper (mm)	Lower (mm)
1	600×600	24φ20	600×500	7φ22	7φ22
2	600×600	24φ14	600×500	7φ24	7φ22
3	600×600	24φ14	600×500	7φ22	7φ22
4	600×600	24φ14	600×500	7φ22	7φ20
5	600×600	24φ14	600×500	7φ20	7φ20
6	600×600	24φ14	600×500	7φ20	7φ18
7	600×600	24φ14	600×500	7φ18	7φ14
8	600×600	24φ14	600×500	7φ16	7φ12
9	600×600	24φ14	600×500	7φ12	7φ10

Table 2: Details of the Factors Applied to the Structure

R	Ω	C_d	I	Site Class
5	3	4.5	1	C

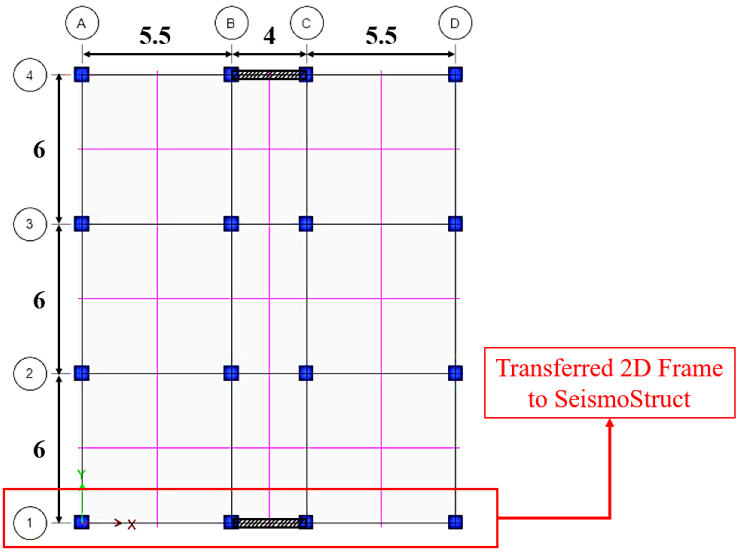

Figure 1: Plan of the 9-Story Structure

2.2. Details of the Nonlinear Modeling of the Structure and Dampers

The reduction in strength and stiffness of the concrete structure under earthquake loading in SeismoStruct is inherently and automatically considered through the nonlinear behavior of materials and their cyclic response. This is achieved by using material models such as con_ma, con_hs, and stl_mp, along with the modeling of structural members using Fiber Sections. The con_ma model (Mander Model) simulates the cyclic nonlinear behavior of concrete, accounting for the degradation of compressive strength and stiffness under cyclic loading for both confined and unconfined concrete. The con_hs model, designed for high-strength concrete, enhances the simulation of cumulative damage and effectively captures the degradation of stiffness and the reduction in energy dissipation capacity under repeated seismic loads. The stl_mp model (Menegotto–Pinto model) is used for reinforcing or structural steel and accurately models the cyclic behavior of steel, including the Bauschinger effect and stiffness degradation.

In SeismoStruct, structural members such as beams and columns are modeled using Fiber Sections, where each fiber is assigned an appropriate material model, such as con_ma for concrete and stl_mp for steel. During nonlinear time-history analysis, earthquake loading is applied to the structure, and the strain in each fiber is computed. Based on the nonlinear behavior of the assigned material, the strength and stiffness of each fiber gradually degrade over time. This results in the progressive reduction of strength and stiffness at the member level and, ultimately, in the entire structure.

As previously mentioned, the 2D structure considered for the study consists of nine stories. Frames along axes 1 and 4 were selected for the installation of rocking shear walls combined with XADAS dampers. The location of the shear wall on axis 1 is between axes B and C. Four CFRP tendons were employed to establish the self-centering mechanism (two tendons on each side of the wall axis). The shear wall has a total height of 28.8 meters from the base level. Naturally, the base of the shear wall is modeled as a pinned connection to simulate the rocking behavior. Perpendicularly, one XADAS damper was placed on each face of the wall (a total of two vertical dampers), and one XADAS damper was installed longitudinally along the wall. The cross-sectional dimensions of the rocking shear wall are 200×3000 mm. Other assumed Parameters for numerical modeling of the structural system are detailed in Table 3.

Table 3: Assumed parameters for numerical modeling of the structural system.

Parameter	Notation	Value	Unit
concrete cover	c	20	mm
concrete modulus of elasticity	E_c	23.5	GPa
concrete compressive strength	f_c'	25	MPa

steel modulus of elasticity	E_s	200	GPa
steel yield strength	f_y	275	MPa
CFRP modulus of elasticity	E_f	240	GPa
CFRP rupture strength	f_f	2750	MPa

2.3. Combined Installation Pattern of Dampers

In this study, after confirming the modeling procedure for the specimens, a combined installation method for dampers in both the longitudinal and perpendicular directions of the wall is proposed. Most previous studies have focused on examining dampers along the longitudinal direction of the wall, and the only existing study on the installation of dampers perpendicular to the wall using brackets is from the research by Vahid-Vahdattalab and Ghandi (2024). In the new method proposed for the present study, two XADAS dampers are installed perpendicularly to the wall on each side using brackets, and one damper is placed along the longitudinal direction of the wall, between the column and the wall. Figure 2 shows the front view and plan of the target structure.

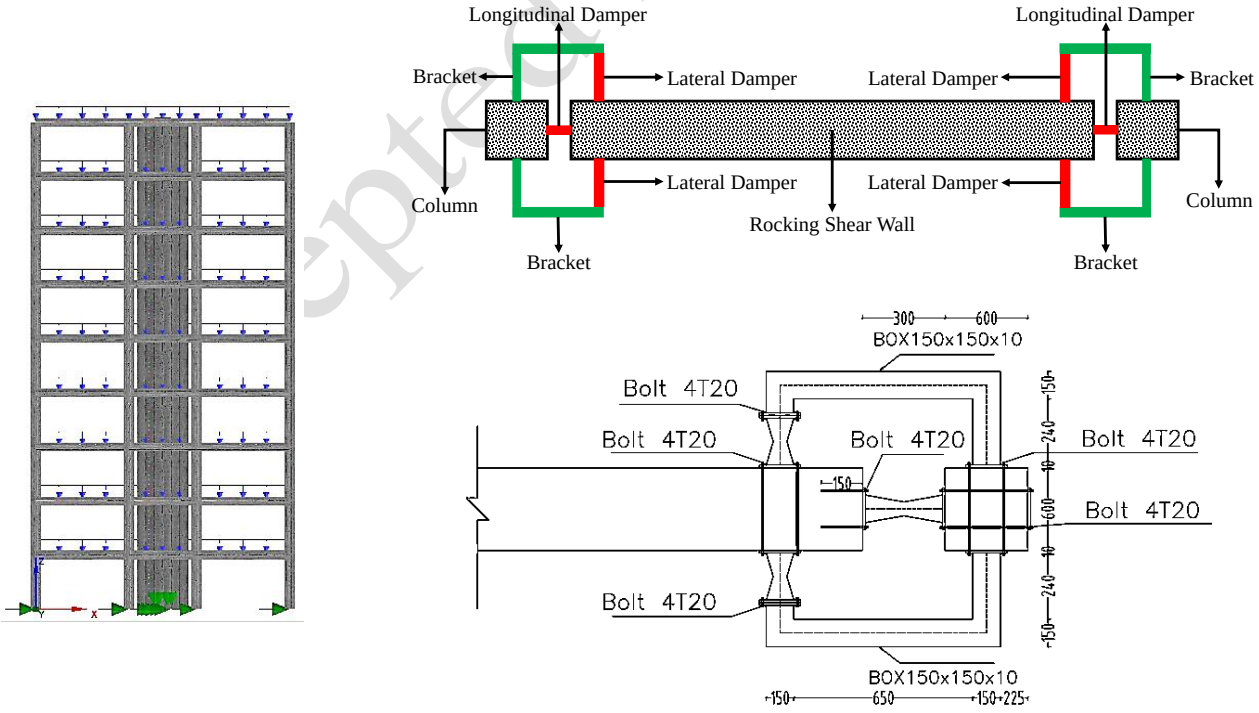

a) Front view b) Plan view and detail

Figure 2: Front view and plan of the target structure.

2.4. Time-History Analysis

After completing the modeling stages, the specimens were subjected to time-history analysis. The selected accelerograms for the specimens include those from Kobe, Kocaeli, Imperial Valley, Landers, Chi-Chi, Northridge, and Tabas earthquakes. It should be noted that these accelerograms were scaled according to the methods outlined in valid codes before being applied to the structure. Specifically, for all accelerograms, a scaling factor was extracted within the range of 0.2T to 1.5T, ensuring that the spectral acceleration of the site does not fall more than 10% below the standard design spectrum. The response spectra of all accelerograms are shown in Figure 3. It is worth mentioning that all the accelerograms used were extracted from the PEER ground motion database, and the specifications of the earthquakes utilized are listed in Table 4. As per the recommendations of reputable codes such as FEMA 356 (FEMA 356, 2000), ASCE 7-10, and ASCE 41-17 (ASCE 41, 2017), which suggest using a minimum of seven ground motion records for performance-based evaluation, this study employs seven earthquake records.

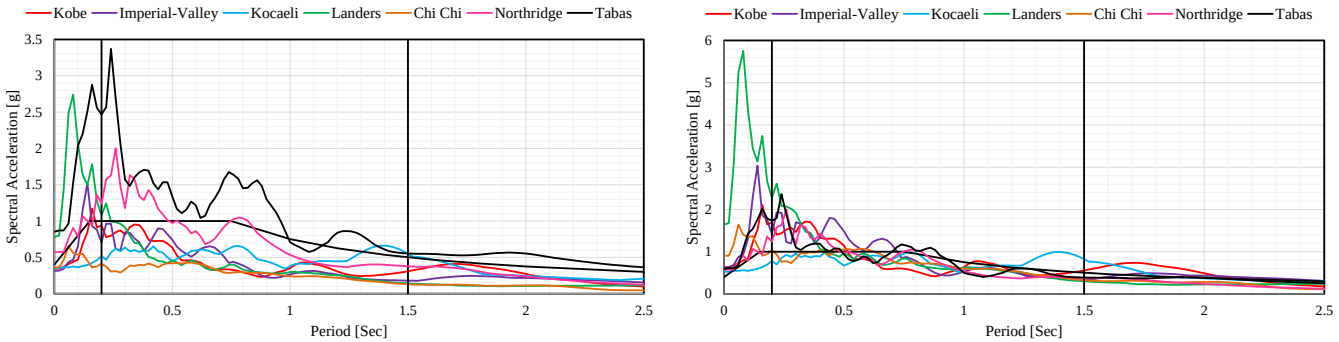

Unscaled spectra of the earthquakes Scaled spectra of the earthquakes

Figure 3: Response spectra of the used accelerograms.

The Kobe, Chi-Chi, Imperial-Valley, Landers, Kocaeli, Northridge, and Tabas earthquakes were selected for time history analysis due to their well-recorded strong ground motions and diverse seismic characteristics. These events cover a range of faulting mechanisms, peak ground accelerations, and site conditions, providing a comprehensive basis for evaluating structural performance. They also represent different tectonic settings from subduction zones to intraplate regions and include both near-fault and far-field ground motions. Their historical significance and impact on seismic code development further justify their selection.

Table 4: Specifications of the Earthquakes for Time History Analysis

Event	Station	Mw	PGA	Scale factor
Kobe	Kakogawa	6.90	0.344	1.8
Imperial-Valley	USGS*	6.40	0.315	2
Kocaeli	Yarimca	7.40	0.349	1.5
Landers	SCE**	7.30	0.780	2.1
Chi-Chi	TCU045+	7.60	0.361	2.5
Northridge	CDMG++	6.69	0.568	1
Tabas	Tabas	7.35	0.597	0.70

* United State Geological Survey
** Southern California Edison
\+ Taiwan Central University
++ California Department of Mines and Geology

3. Reference Study and Verification

The present research involves the development of a numerical analysis framework for studying the parametric behavior of rocking concrete walls with XADAS dampers under static cyclic loading. This effort extends toward their application in concrete moment frames designed according to the ASCE7-10 seismic code, using time-history analysis under at least seven earthquake records to determine the required plastic capacity of the dampers for structural performance control. In any research study, one of the key principles is the validation of the finite element modeling process. Since XADAS dampers have not previously been used in combination with rocking shear walls in any prior studies, the validation in this research is conducted in two parts. The first part involves validating the rocking shear wall (RSW) based on the experimental investigation by Preti et al. (2009), while the second part focuses on validating the XADAS damper using the study by Chukka and Krishnamurthy (2020). A comparison of the cyclic responses of the experimental and numerical models is illustrated in Figure 4. For more detailed information, refer to the study by Vahid-Vahdattalab and Ghandi (2024).

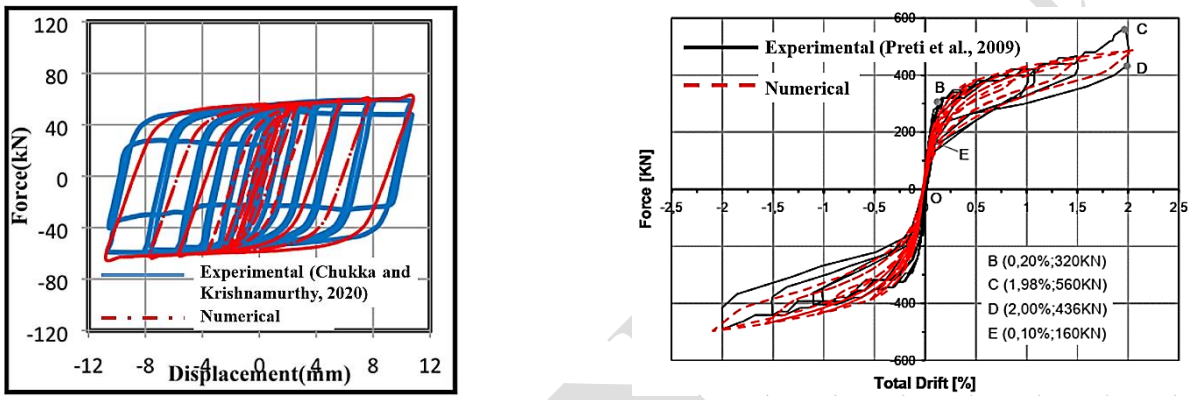

a) XADAS Damper b) RSW

Figure 4: Comparison of the cyclic response of the experimental and numerical models of XADAS damper and RSW (Vahid-Vahdattalab and Ghandi, 2024).

4. Parametric Studies

The primary objective of this study is to investigate the interaction between the frame and the rocking shear wall, calibrate the post-tensioning force of the CFRP tendon, and determine the optimal damper area required. Initially, the post-tensioning force of the CFRP tendon is calibrated using a trial-and-error method through the analysis of a frame equipped with a rocking shear wall without dampers.

Table 5: Calibration Process for CFRP Tendon Post-Tensioning Force

Post-Tensioning Force (kN)	Base Shear (kN)	Residual Displacement
10000	1000	No
500	1300	No
300	1400	No
150	1400	Yes
175	1400	No
160	1400	No
155	1400	Yes

The progression toward the optimal post-tensioning force in the tendons to achieve zero residual displacement is reported in Table 5. As indicated in the table, the minimum force required to simultaneously achieve maximum base shear and zero residual displacement is 160 kN. This force was applied to each of the simulated tendons.

It is evident that applying a force greater than the required value could either:

1- Prevent the wall from maintaining its rocking behavior, consequently reducing the base shear.

2- Result in residual displacement, compromising the system's self-centering mechanism.
It is important to note that zero residual displacement is considered a measure of assurance for the self-centering capability of the system. In the maintenance of the parametric study, the post-tensioning force of the tendons has been kept constant throughout the analyses. Additionally, the effect of the damper cross-sectional area, which increases proportionally with M_p, has been examined on the displacement, drift, acceleration, and the structural safety factor against overturning.

4.1. Effect of Damper Cross-Sectional Area on Structural Displacement

In this part of the study, the influence of different damper cross-sectional dimensions, including 60×20, 60×40, 60×60, 70×20, 70×40, and 70×60 mm, on the story displacements under various earthquake records is examined. Subsequently, after calculating the structural drift in the next section, these results are compared. It is noteworthy that in rocking structures, a reduction in displacement does not necessarily lead to a decrease in drift. Therefore, an optimal and acceptable response is one that simultaneously reduces both displacement and drift. To achieve this, the plastic moment of all dampers is calculated using the Eq. (2).

$$M_p = Zf_y \tag{2}$$

Then, the relationship between max roof displacement (U) variation and plastic moment across all earthquake records is analyzed. The trend of this relationship is illustrated in Figure 5. In the Eq. (1), M_p represents the plastic moment, Z is the plastic section modulus, and f_y is the yield stress of the steel. Additionally, the displacement values corresponding to each earthquake are reported in Table 6.

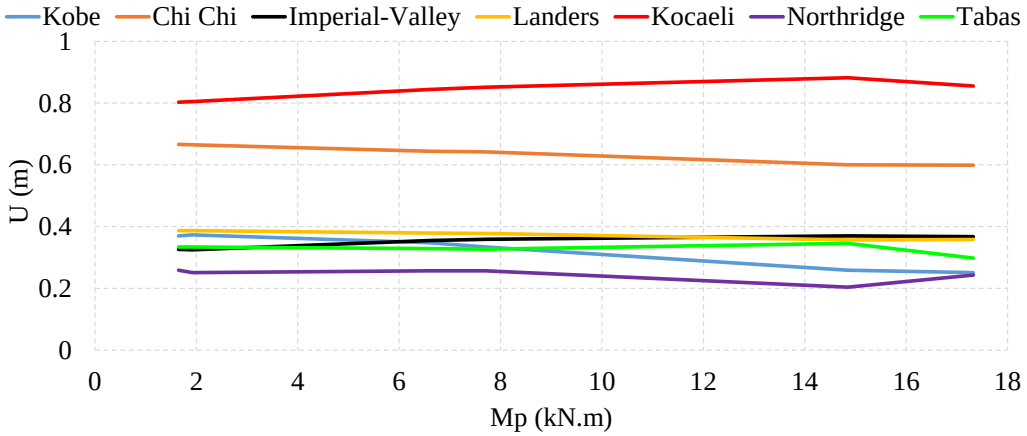

Figure 5: The Trend of Displacement Variations with Plastic Moment

Table 6: Numerical values of the maximum displacement variation trend with plastic moment for each earthquake record.

	b (mm)*	h (mm)**	Mp (kN.m)	U_{max} (m)						
				Kobe	Chi-Chi	Imperial-Valley	Landers	Kocaeli	Northridge	Tabas
F	-	-	0	0.26	0.60	0.38	0.42	0.92	0.24	0.44
FWTD1	60	20	1.65	0.37	0.67	0.32	0.39	0.80	0.26	0.33
FWTD2	70	20	1.925	0.37	0.66	0.32	0.39	0.80	0.25	0.33
FWTD3	60	40	6.6	0.35	0.64	0.35	0.38	0.84	0.26	0.33
FWTD4	70	40	7.7	0.33	0.64	0.36	0.38	0.85	0.26	0.33
FWTD5	60	60	14.85	0.25	0.60	0.37	0.36	0.88	0.20	0.35
FWTD6	70	60	17.325	0.25	0.60	0.37	0.36	0.85	0.24	0.30

F = Bare Frame
FWCD = Frame + Wall + Tendon + Damper
*** Damper section width**
**** Damper section height**

As shown in Figure 5, in the Kobe, Chi-Chi, Landers, Northridge, and Tabas earthquakes, with maximum accelerations of 0.62g, 0.9g, 1.64g, 0.57g, and 0.6g (scaled), respectively, the maximum displacement of the structure decreases by 47.41%, 11.18%, 8.10%, 6.58%, and 12.08% with the increase in the damper cross-sectional area. However, in the Imperial-Valley and Kocaeli earthquakes, with maximum accelerations of 0.63g and 0.52g (scaled), this trend is different, and with the increase in the damper cross-sectional area, the displacement of the structure increases by 12.58% and 6.47%, respectively. The clear reason for this is the rocking nature of the shear wall, and as previously mentioned, in a rocking system, an increase in the damper cross-sectional area does not necessarily result in a reduction of displacement.

4.2. Effect of Damper Cross-sectional Area on Structural Drift

After examining the effect of the damper cross-sectional area on the displacement of the structure, this section of the study investigates the impact of the mentioned parameter on the structural drift. The drift behavior of structures with a rocking system, unlike displacement, follows a general trend of increase or decrease proportional to the cross-sectional area. That is, with an increase in the damper's cross-sectional area, the corresponding drift decreases, and with a decrease in the cross-sectional area, the drift increases. Therefore, by considering both the displacement and drift results, the cross-sectional area of the damper that simultaneously reduces both the displacement and drift of the structure will be considered optimal. The corresponding diagram of the plastic moment and the structural drift is shown in Figure 6. It should be noted that the numerical values of the maximum drift of the structure corresponding to the applied earthquakes are provided in Table 7.

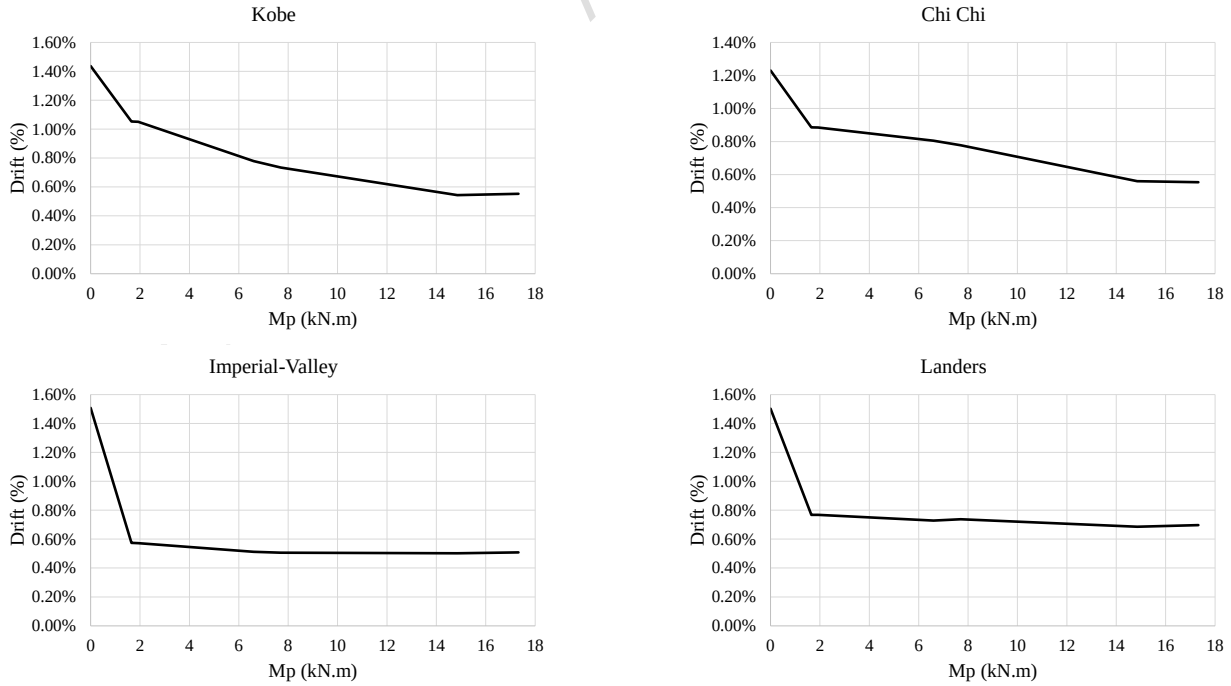

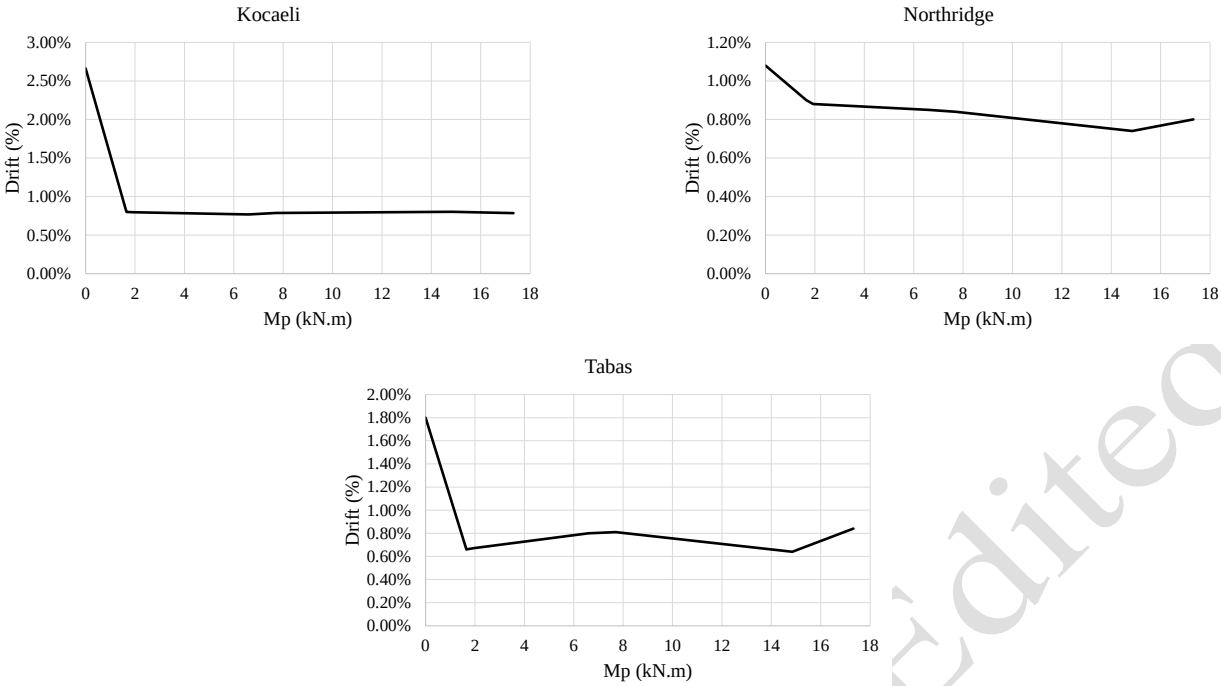

Figure 6: The trend of drift variation with plastic moment for each earthquake.

Table 7: Numerical values of the drift variation trend with plastic moment for each earthquake.

			Drift (%)						
			Kobe	**Chi-Chi**	**Imperial-Valley**	**Landers**	**Kocaeli**	**Northridge**	**Tabas**
	frame*		1.44%	1.23%	1.51%	1.50%	2.66%	1.08%	1.80%
Damper Section (mm)	**60**	**20**	1.05%	0.89%	0.57%	0.77%	0.80%	0.90%	0.66%
	70	**20**	1.05%	0.88%	0.57%	0.77%	0.80%	0.88%	0.67%
	60	**40**	0.78%	0.80%	0.51%	0.73%	0.77%	0.85%	0.80%
	70	**40**	0.73%	0.78%	0.51%	0.74%	0.79%	0.84%	0.81%
	60	**60**	0.54%	0.56%	0.50%	0.69%	0.80%	0.74%	0.64%
	70	**60**	0.55%	0.55%	0.51%	0.70%	0.79%	0.80%	0.84%

* The term of frame, refers to bare frame.

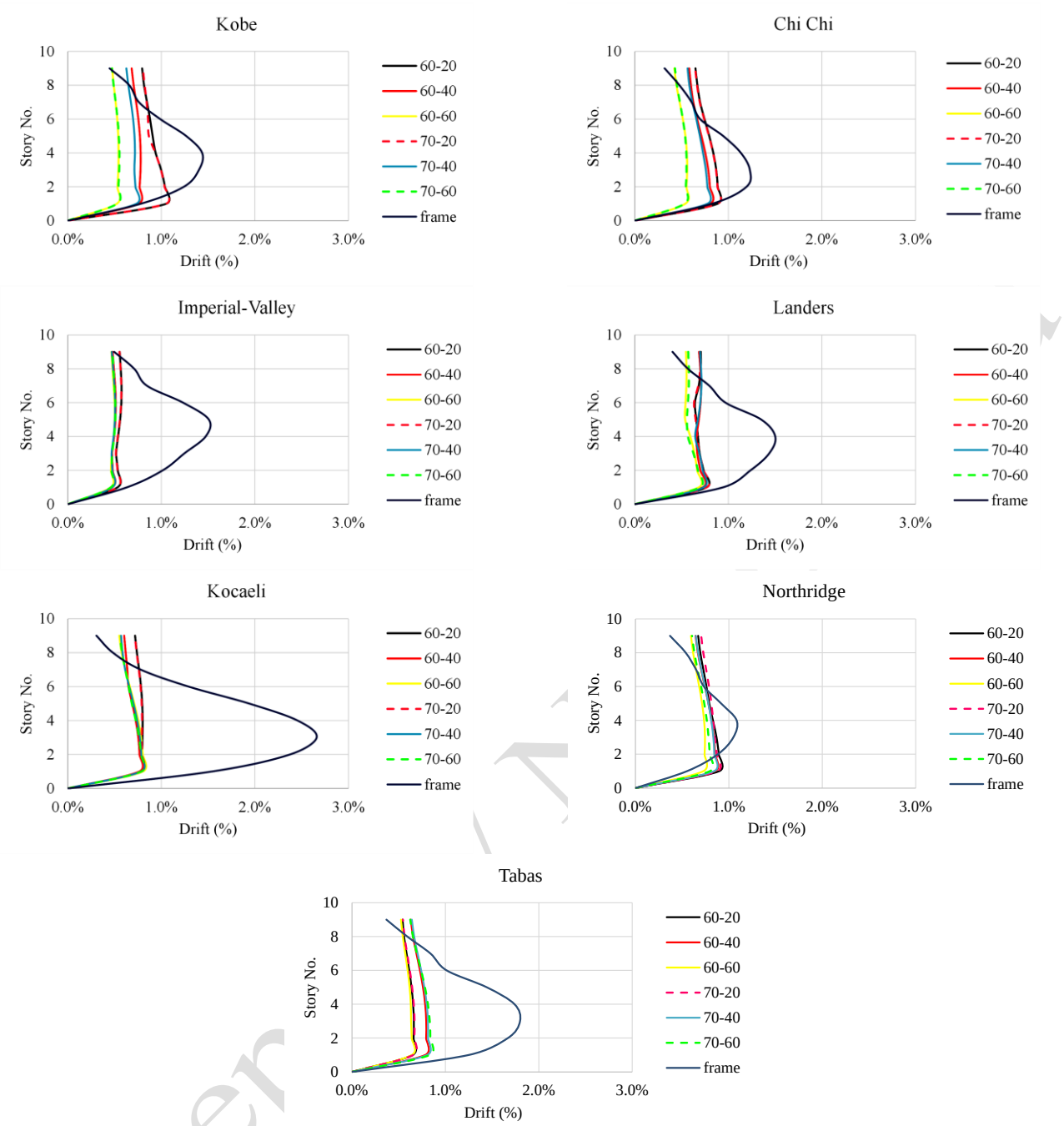

Figure 7: Drift distribution trend across the stories.

By reviewing Table 7 and Figures 6 and 7, it is evident that the maximum drift occurs at the first floor due to all earthquakes, and the greatest reduction in drift due to the use of a damper with a cross-sectional area of 60×40 mm is 245.45% under the Kocaeli earthquake. However, in general, the damper with a cross-sectional area of 60×60 mm shows optimal performance. The resistant moment of the XADAS damper system added to the structure has a moment resistance to total overturning moment ratio of 0.87, 0.94, 1.02, 0.9, and 0.91, respectively, for the Kobe, Chi-Chi, Imperial-Valley, Kocaeli, and Landers earthquakes. Therefore, an average value of 0.93 can be considered for the design of these types of dampers.

4.3. Effect of the damper's cross-sectional area on the ratio of the resisting moment to the overturning moment

One of the important parameters that should be analyzed in the recorded responses of the structure is the distribution of dampers on both sides of the wall, which is closely related to M_p. For this purpose, the shear

force around the damper axis (denoted V_3) for each damper on one side of the wall is recorded, and then the shear forces of all dampers on one side are summed. It is evident that if the damper distribution on both sides of the wall is optimal, the left side shear force V_3L will approximately equal the right side shear force V_3R. The resistant moment of the dampers (M_R^D) is calculated using the Eq. (3).

$$M_R^D = V_3(side\ dampers) \times L_w \quad (3)$$

In the Eq. (3), L_w represents the length of rocking shear wall. Then, the graph showing the ratio of the resistant moment of the damper to the overturning moment of the earthquake with respect to M_p is plotted, as shown in Figure 8. The corresponding numerical values are provided in Table 8.

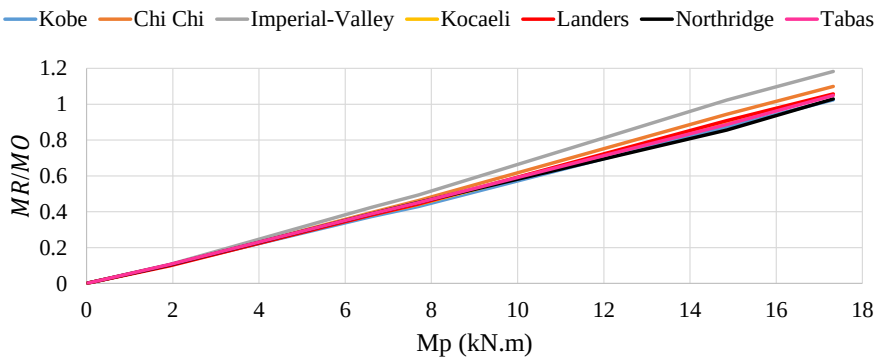

Figure 8: Trend of the ratio of the damper's resistant moment to the earthquake's overturning moment with the plastic moment.

Table 8: Numerical values of the trend of changes in the ratio of the damper's resistant moment to the earthquake's overturning moment with the plastic moment.

M_p (kN.m)	Kobe	Chi-Chi	Imperial-Valley	Kocaeli	Landers	Northridge	Tabas
1.65	0.09	0.09	0.09	0.09	0.08	0.09	0.09
1.92	0.10	0.10	0.11	0.10	0.10	0.10	0.11
6.6	0.37	0.40	0.42	0.38	0.38	0.39	0.39
7.7	0.43	0.46	0.49	0.44	0.44	0.45	0.45
14.85	0.87	0.94	1.02	0.90	0.91	0.86	0.89
17.32	1.02	1.10	1.18	1.05	1.06	1.03	1.05

By examining Figure 8 and Table 8, it is evident that as the damper cross-sectional area increases, leading to an increase in M_p, the safety factor of the structure against overturning also increases. The range of variations in this safety factor indicates that this behavior is almost independent of the type of earthquake, and in all conditions, the use of dampers will increase the safety factor of the structure against overturning. As observed, the changes in the resistant moment to the overturning moment ratio for larger or equal dampers (≥60×60 mm) are negligible with the increase in the plastic capacity of the damper. Therefore, this design can be considered as an optimal design for determining the damper capacity.

4.4. Effect of Damper Cross-Sectional Area on Structural Acceleration

Unlike their fixed-base counterparts, rocking shear walls, due to the oscillations they experience during their operation, cause noticeable changes in the acceleration of the structural floors during an earthquake. It is evident that the acceleration generated due to the oscillations of the rocking system is combined with the inherent acceleration of the structure. Therefore, in such systems, reducing the overall acceleration of the structure through the use of dampers is of particular importance. To investigate the effect of the damper's

cross-sectional area on the overall acceleration of the structure, the acceleration distribution curves at the story levels have been plotted as shown in Figure 9.

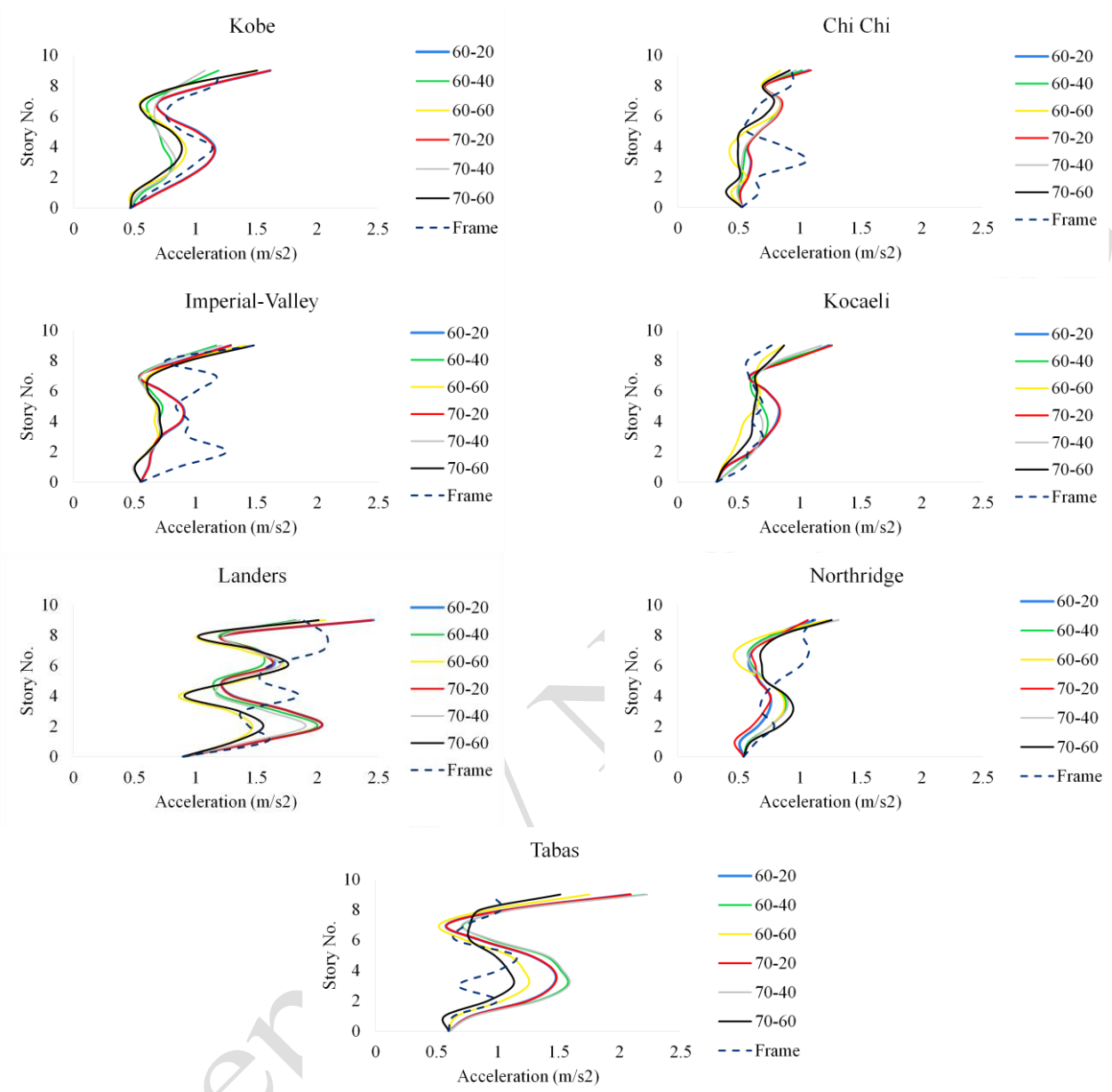

Figure 9: Acceleration Distribution at Story Levels.

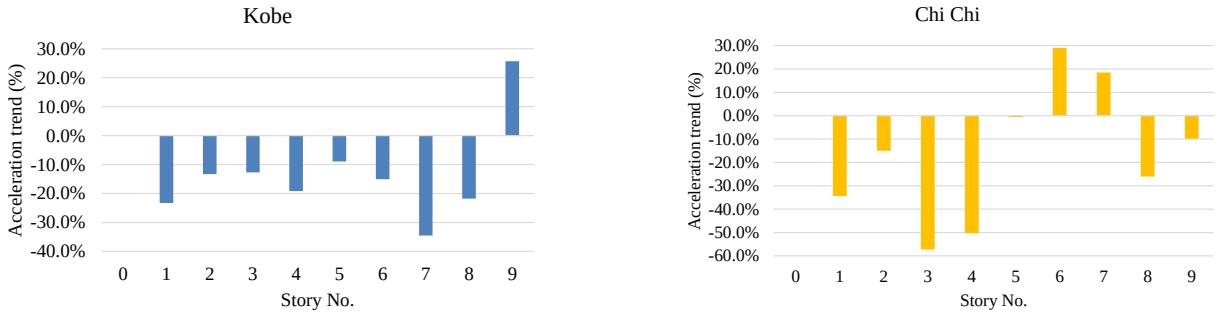

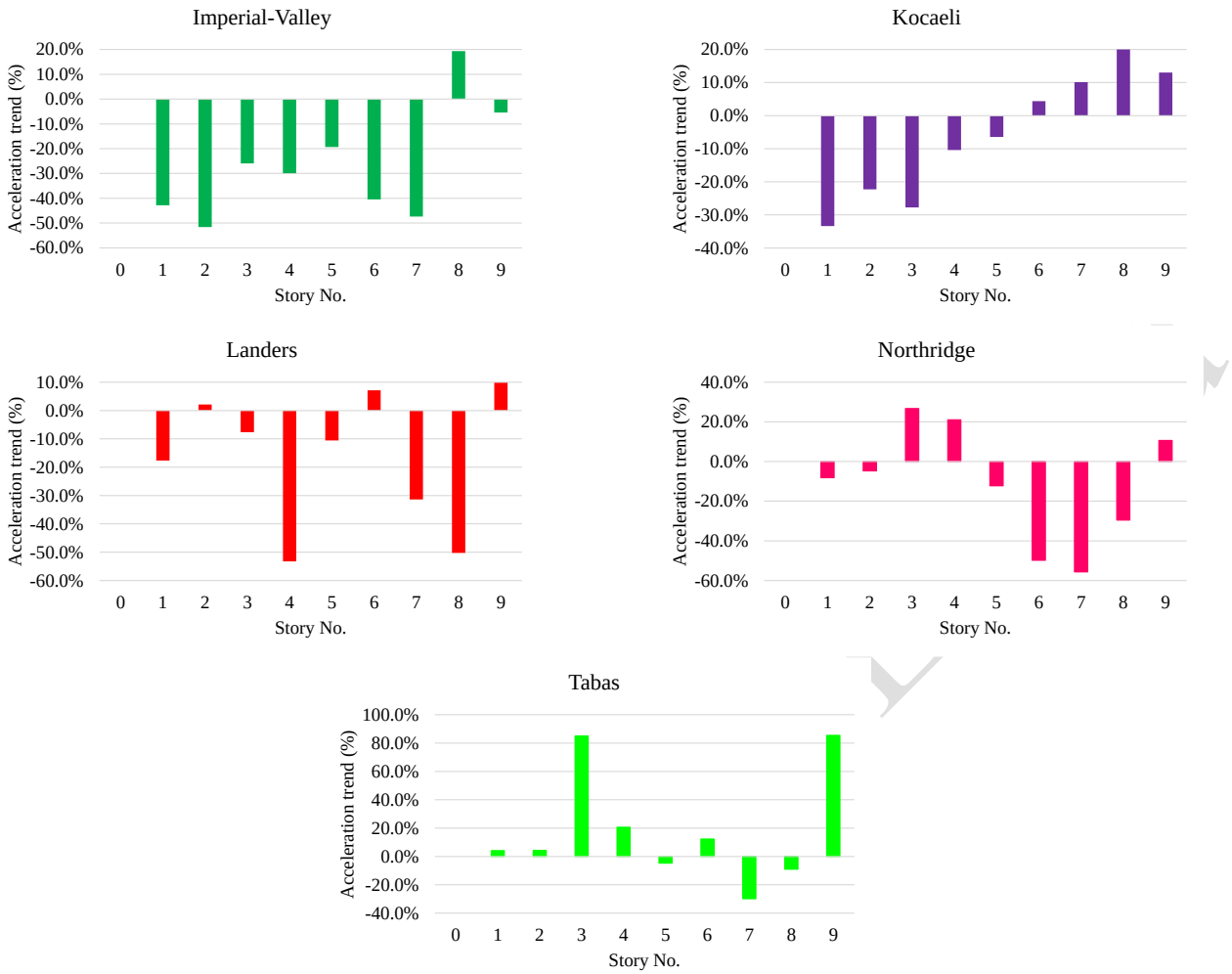

Figure 10: Acceleration Change Pattern of the Shear Wall Structure with Damper of 14.85 kN.m Capacity Compared to the Base Frame Structure.

By examining the curves in Figures 9 and 10, it can be concluded that, firstly, the use of dampers generally leads to a reduction in the structure's acceleration by an average of 10 to 50 percent in the lower two-thirds of the total height of the structure. However, it can be stated that under the effect of all the earthquake records in the current analysis, the upper one-third of the shear wall structure with the damper experienced an average acceleration increase of 30 percent. In other words, there is no direct and predictable relationship between the distribution of displacement and acceleration in the height of the shear wall structure with the damper due to the nonlinear behavior of the dampers and the self-centering of the tendons, which can be explained as follows:

1. Incompatibility between the natural frequency of the structure and the characteristics of the damper: Dampers are designed to perform optimally in the frequency range of the dominant mode of the shear wall system. If the frequency of the earthquake excitation is close to the natural frequency of the shear wall structure, the damper's performance will become irregular in terms of force and deformation distribution along the height, leading to excessive energy being imposed on the damper beyond its capacity, which results in failure and intensified structural vibrations.
2. Irregular interaction between the structure and the damper: The occurrence of complex phenomena, such as resonance, could be one of the factors that increases acceleration even with the use of a damper. While dampers generally reduce structural drift, they can simultaneously cause localized increases in acceleration due to redistribution of accelerations as a result of these phenomena.

3. Earthquake energy-to-damper ratio: Another possible reason for the local increase in acceleration despite the use of dampers is the varying ratio of seismic energy to the damper's energy absorption capacity. In other words, one of the dominant factors in choosing the damper capacity, in addition to its ability to control deformation and self-centering, is its energy absorption capacity relative to the seismic energy of different earthquakes. This aspect could be explored in future research.
4. Type of earthquake and its characteristics: Generally, earthquakes with high acceleration or frequency lead to increased structural acceleration. Therefore, even with the use of a damper, due to its misalignment with the changing, nonlinear frequency of the earthquake, the acceleration might increase.

In summary, it can be concluded that, overall, the use of dampers significantly reduces the acceleration of the shear wall structure compared to the base frame structure. The greatest reduction occurs with the target damper (60×60 mm) with a capacity of 14.85 kN.m under the Chi Chi earthquake, which amounts to 58% in the third floor (lower two-thirds). In contrast, the highest increase in acceleration also occurs under this acceleration record, amounting to 30% on the sixth floor (upper one-third).

4.5. Evaluation of the Performance of a Structure Equipped with Dampers in Reducing Structural Drift

The evaluation of lateral displacement or drift in a structure is of particular importance due to the nature of the rocking shear wall. In this study, the drift response of the moment-resisting frame without dampers and the rocking system under the effect of seven earthquake records was first assessed. Then, it was compared with the response of the system with dampers added. The drift response curve for the structure with the rocking system for the seven earthquake records is shown in Figure 11. In selecting the target damper, it was ensured that the drift response of the structure had the minimum value among the available options for the damper cross-section. Among the selectable options, the 60×60 cross-section is the only one that records the minimum drift.

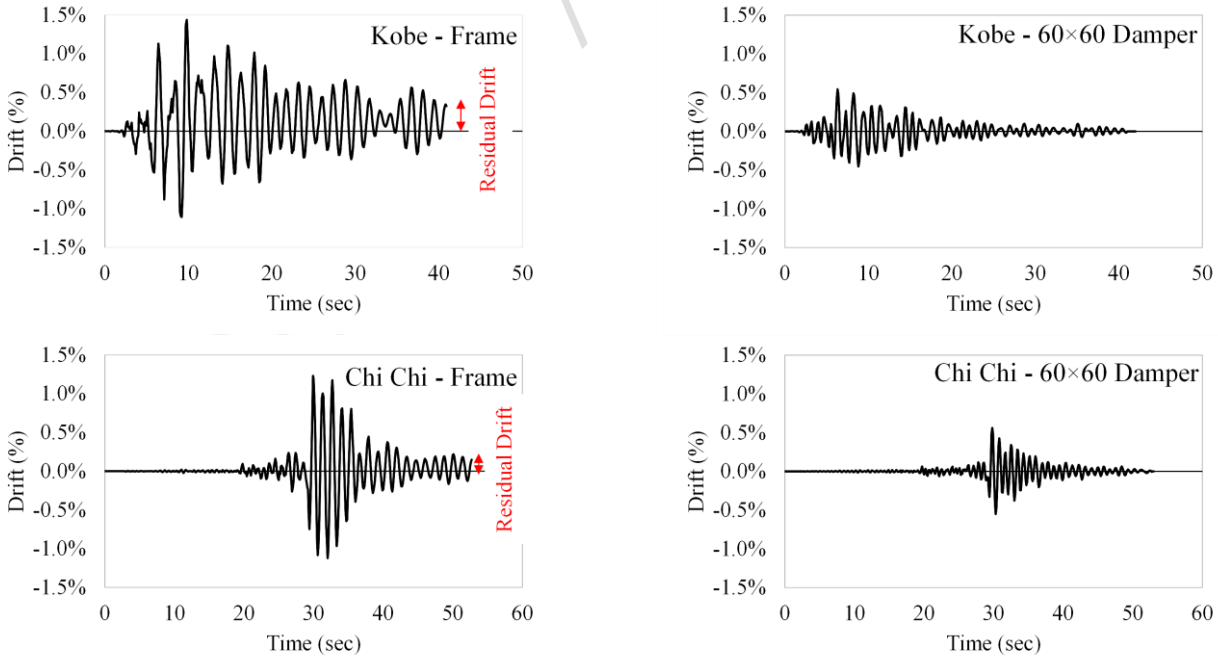

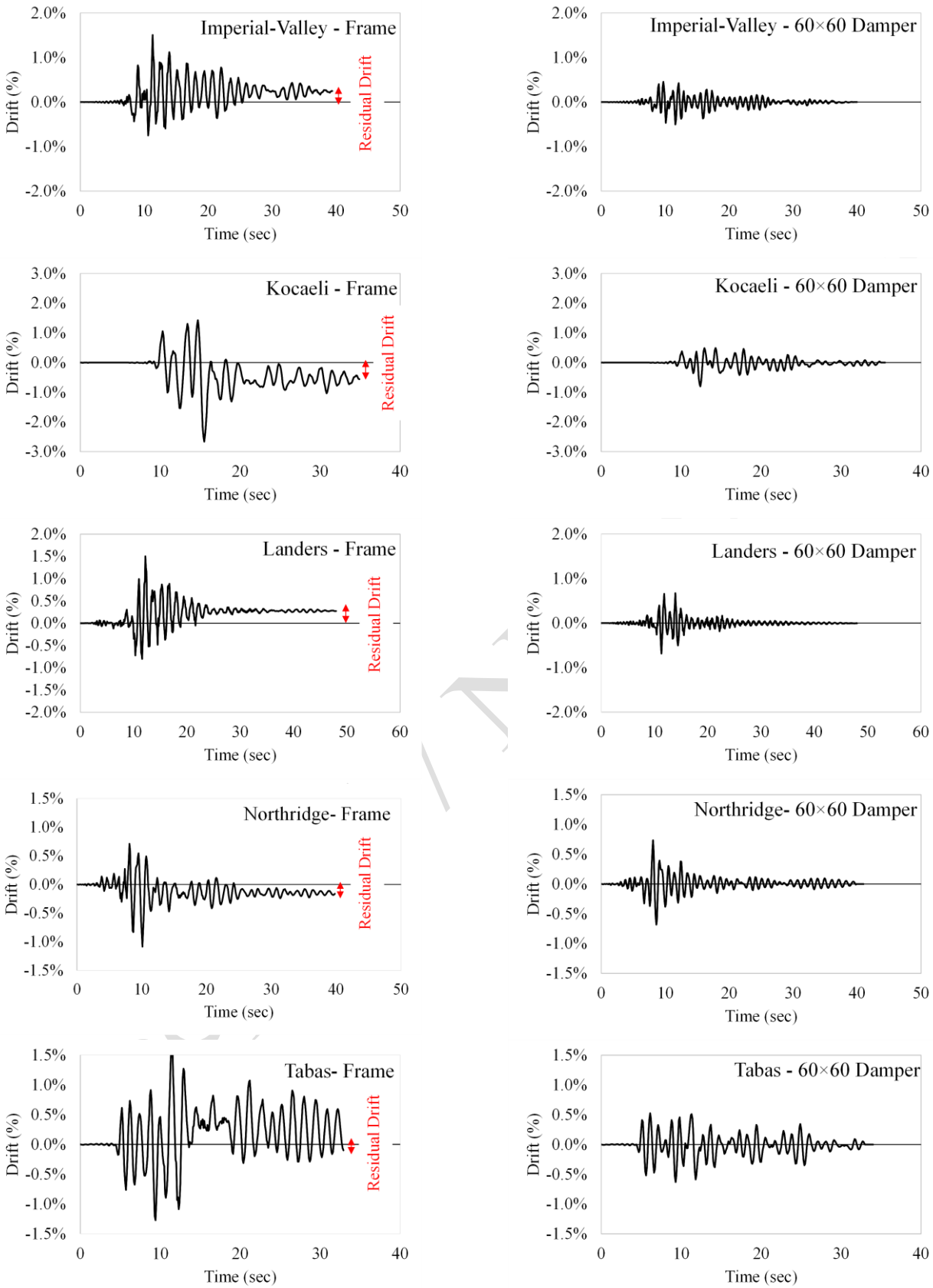

Figure 11: Time History Response of the Structures Drift.

By examining the curves of Figure 11, it can be concluded that adding dampers to the rocking system not only significantly reduces drift but also reduces residual drift and increases damping. The maximum drift of the structure without a damper (moment-resisting frame) and the rocking system under the Kobe, Chi-

Chi, Imperial-Valley, Kocaeli, Landers, Northridge, and Tabas earthquakes are 1.44, 1.23, 1.51, 2.66, 1.5, 1.08, and 1.80 percent, respectively. Moreover, the reduction in drift of the structure due to adding dampers to the rocking system under the aforementioned earthquakes is 166.67%, 123.64%, 202.0%, 245.45%, 117.40%, 45.94%, and 181.25%, respectively. It should be noted that according to the conducted studies, adding any cross-sectional area of the damper does not improve the drift performance of the structure. Cross-sectional areas of 60×20 and 70×20 mm have practically no effect on reducing drift, and in some cases, the 70×60 mm cross-section performs almost 2% worse than the 60×60 cross-section.

5. Conclusions

This study investigated the seismic interaction of a concrete moment-resisting frame with a rocking shear wall equipped with longitudinal and perpendicular combined dampers. Parametric studies and nonlinear time-history analyses highlighted the critical influence of post-tensioning force on the self-centering performance of the system. An optimal post-tensioning force of 160 kN per CFRP tendon was identified, providing a balance between energy dissipation and restoring capacity. Excessive force suppressed rocking action, while insufficient force led to residual displacements, emphasizing the importance of careful calibration.

Results also demonstrated a nonlinear relationship between damper size and structural response. Unlike fixed-base systems, increased damper area did not consistently reduce displacement, although larger dampers generally improved drift performance. A 60×60 mm damper provided an effective balance between displacement control and overturning stability. Additionally, placing dampers symmetrically on both sides of the wall significantly enhanced overturning resistance, highlighting the role of balanced energy dissipation in optimizing the seismic performance of rocking wall systems.

- The calibration process for the CFRP tendon post-tensioning force revealed that a value of 160 kN per tendon was optimal for ensuring both maximum base shear capacity (1400 kN) and zero residual displacement, thereby maintaining the self-centering capability of the rocking shear wall. Forces below 155 kN resulted in permanent displacements, while higher values such as 10000 kN suppressed the rocking behavior and significantly reduced base shear to 1000 kN, indicating a loss of energy dissipation capacity. Therefore, the post-tensioning force of 160 kN was selected for all subsequent models to provide an effective balance between self-centering capability and structural energy dissipation.
- The influence of damper cross-sectional area on structural displacement was evaluated for six different damper sizes ranging from 60×20 mm to 70×60 mm, corresponding to plastic moments (M_p) from 1.65 kN.m to 17.33 kN.m. Results showed that increasing the damper area reduced maximum roof displacement in five out of seven ground motions. The most notable reductions occurred in the Kobe (–47.41%), Chi Chi (–11.18%), Landers (–8.10%), Northridge (–6.58%), and Tabas (–12.08%) records, as damper plastic moment increased from 0 to 17.33 kN.m. However, in the Imperial-Valley and Kocaeli earthquakes, displacements increased by 12.58% and 6.47%, respectively, indicating that larger damper sections may adversely affect performance under certain excitation patterns. These variations reflect the nonlinear interaction between damping and rocking mechanisms, where increased damper stiffness can unintentionally limit beneficial rocking motion. Among all tested configurations, the 60×60 mm damper (M_p = 14.85 kN.m) provided the most favorable balance between displacement control and structural stability across different seismic inputs.
- In terms of structural drift, results indicated a consistent reduction as the damper cross-sectional area increased. For example, the maximum drift decreased from 2.66% to 0.77% (a 245.45% reduction) under the Kocaeli earthquake when increasing damper dimensions from 60×20 mm to 60×40 mm. Across all records, the 60×60 mm damper consistently provided the most favorable drift control, achieving average drift reductions of over 40% compared to the bare frame configuration. This

performance indicates its suitability as the optimal section in terms of both displacement and drift control. Furthermore, analysis of the damper's contribution to overturning resistance showed that the moment resistance-to-overturning moment ratio ranged between 0.87 and 1.02 for the tested earthquake scenarios, with an average value of 0.93. This ratio demonstrates the damper's significant role in stabilizing the structure against overturning and can serve as a practical benchmark for the seismic design of similar damping systems.

- The distribution of dampers on both sides of the wall was evaluated by comparing the total shear force around the damper axis (V_3) on each side. A balanced shear response (i.e., $V_3L \approx V_3R$) indicated effective damper placement. The resistant moment of dampers ($M_R^D = V_3 \times L_w$) was used to compute the resistant-to-overturning moment ratio for each configuration. Results demonstrated that increasing the plastic moment (M_p) of dampers from 1.65 kN.m to 17.32 kN.m improved the overturning safety factor from approximately 0.08 to over 1.18, indicating up to a 14-fold increase in stability across various seismic inputs. It was also observed that for $M_p \geq 14.85$ kN.m (corresponding to damper sizes of 60×60 mm and above), the increase in the safety factor began to plateau, suggesting a saturation effect. Therefore, damper designs with M_p around 14.85 kN.m (e.g., 60×60 mm section) were identified as optimal, offering substantial overturning resistance without unnecessary overdesign. Additionally, the observed trends were consistent across all seven earthquake records, indicating that the effectiveness of this configuration is largely independent of ground motion characteristics.
- Analysis of Figures 9 and 10 indicates that the incorporation of dampers generally resulted in a 10–50% reduction in floor accelerations across the lower two-thirds of the structure's height. Notably, the most significant reduction 58% was observed on the third floor using a 60×60 mm damper with a plastic moment capacity of 14.85 kN.m under the Chi-Chi earthquake. However, a 30% increase in acceleration was recorded in the upper one-third of the structure under the same earthquake, highlighting the complex interaction between damping mechanisms and structural dynamics.
- The study confirmed the critical role of lateral drift evaluation in assessing the seismic performance of rocking systems. Comparing a moment-resisting frame with and without dampers under seven earthquake records revealed that adding dampers significantly improved performance. Maximum interstory drift without dampers reached up to 2.66% (Kocaeli), while the incorporation of dampers reduced drift by up to 245.45%. Other notable reductions included 202.0% (Imperial-Valley), 181.25% (Tabas), 166.67% (Kobe), 123.64% (Chi-Chi), 117.40% (Landers), and 45.94% (Northridge). Among all damper configurations, the 60×60 mm damper with a plastic moment capacity of 14.85 kN.m achieved the most consistent and effective drift reduction. Smaller dampers (60×20 mm, 70×20 mm) had minimal impact, while the larger 70×60 mm option, despite a slight capacity increase, performed about 2% worse in terms of drift control. Overall, the 60×60 mm damper provided the best balance between drift mitigation and structural efficiency for the rocking shear wall system.

6. References

ASCE (American Society of Civil Engineers), (2010). "Minimum design loads for buildings and other structures", Standard ASCE/SEI 7-10.

American Society of Civil Engineers (ASCE), (2017). "Seismic evaluation and retrofit of existing buildings (ASCE/SEI 41-17) ", Reston, VA: ASCE.

Aydin, E., Noroozinejad Farsangi, E., Öztürk, B., Bogdanovic, A. and Dutkiewicz, M., (2019). "Improvement of building resilience by viscous dampers", *Resilient structures and infrastructure*, pp.105-127, https://doi.org/10.1007/978-981-13-7446-3_4.

Canadian Standards Association. (2014). "Design of concrete structures (CSA A23. 3-14)", CSA, Mississauga, ON, Canada.

Cetin, H., Aydin, E. and Ozturk, B., (2019). "Optimal design and distribution of viscous dampers for shear building structures under seismic excitations", *Frontiers in Built Environment*, 5, p.90, https://doi.org/10.3389/fbuil.2019.00090.

Chen, Y., Xu, R., Wu, H. and Sheng, T., (2022). "A multi-objective design method for seismic retrofitting of existing reinforced concrete frames using pin-supported rocking walls", *Frontiers of Structural and Civil Engineering*, 16(9), pp.1089-1103, https://doi.org/10.1007/s11709-022-0851-z.

Chukka, N.D.K.R. and Krishnamurthy, M., (2020), October. "Seismic performance assessment of structure with hybrid passive energy dissipation device", In *Structures* (Vol. 27, pp. 1246-1259), Elsevier, https://doi.org/10.1016/j.istruc.2020.07.038.

Ding, M., Shi, Q., Wang, B. and Wang, Q., (2024). "Novel pre-pressure friction spring RC rocking column with enhanced segment: Practical design and numerical investigation", *Journal of Building Engineering*, 96, p.110444, https://doi.org/10.1016/j.jobe.2024.110444.

ETABS, C, (2016). "Integrated building design software Version 16.2.0", Berkeley, USA: Computers and Structures.

Fang, C., Qiu, C., Wang, W. and Alam, M.S., (2023). "Self-centering structures against earthquakes: a critical review", *Journal of Earthquake Engineering*, 27(15), pp.4354-4389, https://doi.org/10.1080/13632469.2023.2166163.

Federal Emergency Management Agency (FEMA), (2000). "Prestandard and commentary for the seismic rehabilitation of buildings (FEMA 356)", Washington, DC: FEMA.

Ghandi, E., Mohammadi Rana, N. and Esmaeili Niari, S. (2025). "Parametric Analysis of Axially Loaded Partially Concrete-Filled Cold-Formed Elliptical Columns Subjected to Lateral Impact Load", *Civil Engineering Infrastructures Journal*, 58(1): 49-70, https://doi.org/10.22059/ceij.2024.364758.1955.

Han, T., Liu, Y., Lu, Y., Wu, W., Sun, T. and Lv, Q., (2023, October). "Design and numerical analysis of Cross-Laminated bamboo (CLB) buildings with different rocking wall configurations", In *Structures* (Vol. 56, p. 105011), Elsevier, https://doi.org/10.1016/j.istruc.2023.105011.

Huang, X., Zhou, Z. and Zhu, D., (2019). "Analytical investigation on lateral load responses of self-centering walls with distributed vertical dampers", *Structural Engineering and Mechanics*, 72(3), pp.000-000, https://doi.org/10.12989/sem.2019.72.3.000.

Huang, L., Qian, Z., Meng, Y., Jiang, K., Zhang, J. and Sang, C., (2023). "Parametric Investigation of Self-Centering Prestressed Concrete Frame Structures with Variable Friction Dampers", *Buildings*, 13(12), p.3029, https://doi.org/10.3390/buildings13123029.

Lv, Q., Han, T., Liu, Y., Ding, Y. and Lu, Y., (2021). "An experimental and analytical study on cross-laminated bamboo rocking walls with friction dampers", *Journal of Renewable Materials*, 9(10), pp.1757-1779, https://doi.org/10.32604/jrm.2021.015536.

Mander, J.B., Priestley, M.J. and Park, R., (1988). "Theoretical stress-strain model for confined concrete", *Journal of structural engineering*, 114(8), pp.1804-1826, https://doi.org/10.1061/(ASCE)0733-9445(1988)114:8(1804).

Menegotto, M., (1973). "Method of analysis for cyclically loaded RC plane frames including changes in geometry and non-elastic behavior of elements under combined normal force and bending", *In Proc. of IABSE Symposium on Resistance and Ultimate Deformability of Structures Acted on by Well Defined Repeated Loads*.

Palnikov, I.S., (2017). "Design and Experimental Investigation of 500kV Current Transformer Seismic Retrofit Utilizing Structure Rocking and Supplemental Damping with Self-Centering", *(Master's thesis, Portland State University)*.

Preti, M., Marini, A., Metelli, G. and Giuriani, E.P., (2009). "Full scale experimental investigation on a prestressed rocking structural wall with unbonded dowels as shear keys", *In Proceedings of the XIII conference Anidis 2009*.

SeismoStruct, S, (2022). "A Computer Program for Static and Dynamic Nonlinear Analysis of Framed Structures".

Vahid-Vahdattalab, F. and Ghandi, E., (2024, October). "HSC-RSW with laterally installed XADAS dampers: Seismic performance", In *Structures* (Vol. 68, p. 107093), Elsevier, https://doi.org/10.1016/j.istruc.2024.107093.

Wang, Y., Zhou, Z., Ge, H., Yao, J. and Xie, Q., (2022). "Experimental validation and numerical simulation of a dual-self-centering variable friction braced frame under strong ground motions", *Journal of Building Engineering*, 56, p.104761, https://doi.org/10.1016/j.jobe.2022.104761.

Xue, D., Bi, K., Dong, H., Qin, H., Han, Q. and Du, X., (2021). "Development of a novel self-centering slip friction brace for enhancing the cyclic behaviors of RC double-column bridge bents", *Engineering Structures*, 232, p.111838, https://doi.org/10.1016/j.engstruct.2020.111838.

Zhang, J., Zhang, M., Liu, X. and Sun, Y., (2024). "Structural behavior of steel tube reinforced resilient RAC shear walls under static cyclic loading", *Journal of Building Engineering*, 90, p.109432, https://doi.org/10.1016/j.jobe.2024.109432.

Zhong, X., Shen, Y., Chen, X., Li, J. and Wang, Y., (2024). "Seismic performance of a novel hemisphere-based rocking hinge realizing self-centering damage-free bridge system", *Engineering Structures*, 298, p.117032, https://doi.org/10.1016/j.engstruct.2023.117032.